Postprint of: Mikielewicz D., Klugmann M., Wajs J., Flow boiling intensification in minichannels by means of mechanical flow turbulising inserts, International Journal of Thermal Sciences, Vol. 65 (2013), pp. 79-91, DOI: 10.1016/j.ijthermalsci.2012.10.002

Manuscript submitted for consideration to publish in International Journal of Thermal Sciences

FLOW BOILING INTENSIFICATION IN MINICHANNELS BY MEANS OF MECHANICAL FLOW TURBULISING INSERTS

Dariusz Mikielewicz, Michał Klugmann, Jan Wajs

Gdansk University of Technology, Faculty of Mechanical Engineering, Department of Energy and Industrial Apparatus, ul. Narutowicza 11/12, 80-233 Gdansk, Poland
Email: Dariusz.Mikielewicz@pg.gda.pl, tel. +48 58 347 2254

ABSTRACT

The work presents the results of experimental investigation on heat transfer in minichannels. Refrigerant R123 was used as a test fluid. Single vertical silver tubes of 380 mm length and 2.3 mm diameter were examined with two variants of turbulising inserts. A wide range of parameters was considered, namely mass flux G = 534 ÷ 3011 kg/(m^{2}s), heat flux q_w = 28.5 ÷ 68.4 kW/m^2, saturation temperature T_{SAT} = 23 ÷ 86 °C and the full range of vapour quality variation (x = 0 ÷ 1). The effect of mass flux and heat flux on heat transfer coefficient was analysed both for the smooth tube and for two turbulisation variants. The results were compared with popular smooth tube correlations. For the case of a smooth tube the M-shape of heat transfer coefficient curve as a function of quality was observed, which is a completely new finding confirmed in the literature only recently. There are some circumstances of similar existence of two heat transfer coefficient maxima also for the tubes with turbulising inserts. The discussion of flow boiling intensification possibilities in minichannels with the use of this method was based on the number of comparisons of the smooth tube and two turbulisation variants for various established parameters.

Keywords: minichannels, flow boiling, turbulisation, flow blocking

1. INTRODUCTION

The techniques of heat transfer improvement (intensification) in conventional applications have been under scrutiny in literature for more than a century and a large number of information was gathered up to now [1]. Generally speaking, the intensification methods can be classified as *passive* (no additional energy have to be supplied) and *active* (additional energy is required). Efficiency of such methods strongly depends on heat transfer conditions and mechanisms which can change from single phase convective heat transfer to the flow boiling.

The active techniques require additional power to obtain the intensification effect. To this group belong for example generation of flow pulsations using magnetic fields to set the flow whirling, etc. [1]. It's acknowledged that the active techniques don't present a significant perspective potential because of technical complications related with applications. Additionally supplying of additional power is in some cases not easy. Passive techniques don't require supply of additional power, but finally always lead to the increased pressure drop.

Placing of varied inserts in the flow (twisted ribbons, coils, fins) is one of the passive heat transfer intensification methods, which on the other hand causes the reduction of channel hydraulic diameter. The most important mechanisms, which lead to the heat transfer improvement are: flow blocking, flow segmentation and secondary flows. Flow blocking increases the pressure drop and leads to the increase of the effects related to viscosity because of the reduction of free space for the flow. It also causes the flow velocity to increase and, in some conditions, the noticeable secondary flow. The secondary flow finally improves the thermal contact between the liquid and the surface by whirls generation and stirring the liquid, which leads to the enlargement of temperature gradient and to increase of the heat transfer coefficient.

Flow boiling is regarded as intense heat transfer case. In spite of the great efficiency of heat exchange during flow boiling, also in this case some attempts of the further improvements can be considered. There are not too many works describing this problem in literature. Present

work describes the influence of turbulising inserts as potential heat transfer intensification possibility. In the considered case an attempt to generate annular geometry was made by introduction into the flow of rectangular cross-section and circular cross-section wires as presented in the table 1. In such way the blocking effect was obtained.

Inner diameter	**2.3 mm**
Turbulising insert 1 (T1) (D_h=0.8449 mm)	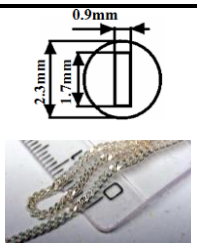
Turbulising insert 2 (T2) (D_h=1.3 mm)	

Table 1. Two variants of turbulising inserts

A useful method of comparing the performance of smooth tubes and the tubes with inserts is to compare them at equal pumping power. That leads to the equation:

$$\left(\dot{V}\Delta p\right)_0 = \left(\dot{V}\Delta p\right) \qquad (1)$$

Expressing adequately the volumetric flow rate and the pressure drop we get the relationship between the resistance coefficients and Reynolds numbers:

$$\left(f\,\mathrm{Re}^3\right)_0 = \left(f\,\mathrm{Re}^3\right) \qquad (2)$$

or in the other way:

$$f_0^{1/3}\,\mathrm{Re}_0 = f^{1/3}\,\mathrm{Re} \qquad (3)$$

Heat transfer intensification coefficient can be defined as a function of heat transfer efficiency increase and pumping power at the same flow rate. This parameter is also used for comparisons between various passive heat transfer intensification techniques at specified pressure drop. It's described by an equation arising from (2), [2]:

$$E = \frac{(Nu / Nu_0)}{(f / f_0)^{1/3}} \qquad (4)$$

where Nu, f, Nu_0 i f_0 are Nusselt's numbers and resistance coefficients for two channel configurations: with the turbulising insert and without it respectively. Resistance coefficient is determined basing on the pressure drop or on the power of the pump.
Intensification efficiency (at constant pumping power) can be expressed as [3]:

$$E_p = \left.\frac{\alpha}{\alpha_0}\right|_{\text{pumpingpower}=\text{const}} \qquad (5)$$

Use of expressions (4) or (5) is possible rather only for single phase flow because the correlations describing the relation between heat transfer coefficient and Reynolds number as well as the relation between resistance coefficient and Reynolds number are required simultaneously. Finding such correlations for the flow boiling is very difficult or even impossible for some conditions. In that case the heat transfer intensification is expressed as heat transferred through the tube in relation to the pumping power for both cases: smooth and turbulised tube. Such methodology is possible and the expression (4) is based on it.

Heat transfer intensification in the channel in flow boiling can be described as the ratio of heat absorbed by the tube in relation to the pumping power, first for the tube with turbulising insert, and second, for the smooth tube of the same diameter, subscript 0, respectively. This method can be used when the qualities in both cases are equal. The expression is:

$$E_x = \left.\frac{\left(\frac{\dot{Q}}{\dot{V}\,\Delta p}\right)}{\left(\frac{\dot{Q}}{\dot{V}\,\Delta p}\right)_0}\right|_{x=const} \qquad (6)$$

If $E_x>1$, the intensification occurs in the examined configuration. Equation (6) is the general expression. The numerator can be interpreted as the net heat possible to be transferred through the channel with intensification. The denominator describes the same for the smooth tube. The compared net effect includes both the quantity of transferred heat and the expenditure of energy needed for the medium pumping.

2. EXPERIMENTAL FACILITY

Figure 1. General view of experimental facility

The experimental rig has been designed as a compact, highly integrated mobile unit. It's main part is a closed loop of a working fluid. The Freon R-123 (Suva) has been chosen because of very convenient saturation temperature: 27.9 ºC under normal conditions. In authors earlier studies experiments in flow boiling were also studied on that facility which were reported in [4]. For that reason here only a brief recapitulation on the experimental details will be presented. Unfortunately R123 is very permeable and aggressive for the most of gaskets (except of PTFE and polyamide), so the issue of the loop tightness presented a challenge prior to the commencement of experiment. The flow of the working fluid is forced by an electrically-powered pump, which is capable to give mass flow ratio up to 200 kg/h and overpressure up to 8 bars. A gear pump has been chosen to avoid any flow pulsations. Adjustment of the mass flow is realized by changing voltage of the pump's power supply or using by-pass. Working medium is pumped from the main tank to the Danfoss mass flowmeter type MASS D1 3 working with MASS 6000 19" IP20 interface. This system, called MASSFLO, gives about 0.3% accuracy. In the present work the mass flow range from 10 to 45 kg/h has been considered. Then the medium goes to the pre-heater, where it obtains appropriate input parameters. Isobaric pre-heating is realized in the stainless steel tube powered by low voltage, high current DC power supply. It provides up to 1.2 kW of heating power which is equivalent to 168 kW/m^2 in terms of heat flux. In this way, the full range of x is possible to be obtained on the test section input. Current, voltage, inlet and outlet temperatures, and pressure are measured on the pre-heater to determine heat flux and x.

Figure 2. Schematic diagram of test facility: 1– main tank; 2 – pump section; 3 – filter/dryer; 4 – mass flowmeters; 5 –pre-heater; 6 – test section; 7 – condenser; 8 – by-pass; 9 – filling valve; 10 – de-aerator

From the pre-heater the medium goes directly to the test section. In this experiment a silver tube of 2.3 mm inner diameter and the length of 38 cm has been used. The working medium flows into the tube with pre-defined x and is heated further to get the expected boiling structures. Heating in test section is realized using low voltage, high current AC power supply and can be adjusted from 0 up to 1 kW of heating power, what corresponds to 364 kW/m^2.

Current, voltage, inlet temperature, inlet pressure, outlet temperature and outlet pressure are measured on the test section to determine heat flux, subcooled liquid temperature, saturation temperature of boiling liquid and pressure drop. As the pressure drop is proved to be non-linear in such small diameters, five additional pressure measurement points were also applied on the tube length to determine the pressure drop shape. The tube wall temperature gradient is measured using the set of 10 K-type thermocouples, soldered directly to the wall. All the data are recorded automatically using PC computer with a data acquisition interface. The measuring system uses a specially developed in-house software TERMOLAB 06. Alternatively, the wall temperature gradient can be visualized using infrared camera, which is especially effective when the critical heat flux is reached. From the test section the fluid goes to the condenser (using cold water) and back to the main tank.

Current, voltage, inlet and outlet temperatures and pressure were measured on the pre-heater to determine a corresponding heat flux and quality x from the appropriate heat balance. From the pre-heater the medium went directly to the test section. The working medium flowed into the tube with a pre-defined quality x and was heated further to get the expected boiling conditions. At the test section again electric current, voltage, inlet temperature, inlet pressure, outlet temperature and outlet pressure were measured to determine the corresponding heat flux, saturation temperature of boiling liquid and pressure drop. Quality was calculated from the heat balance, whereas the heat transfer coefficient was determined as a ratio of heat flux to the local temperature difference between the wall and saturation condition.

2.1. Uncertainty of measurements

Experimental uncertainty was determined using the sequential perturbation method (Moffat [14]) of error analysis. This method allows to determine a total experimental error by including errors originating from individual sources into general database and averaging it using a root sum square method (RSS).

An error analysis was executed automatically for each data series. It was implemented into the spreadsheets used for data reduction. Also the heat balance was examined automatically for each case. For the case of convective heat transfer it was based on specific heat and temperature difference. For flow boiling it was based on enthalpy difference. It was proved that an average uncertainty of heat transfer coefficient determination didn't exceeded 5%. An uncertainty of pressure measurement for single phase flow was at the level of 400 mbar.
For single data series an extremely large errors were observed, even exceeded 100%. This occurs for particularly large heat fluxes, when the dryout appears. This phenomenon neither was the subject of the present work nor was included into data reduction procedure, so such series wasn't taken into account. Details are presented in Table 2.

Measured quantity	**Uncertainty**
Temperature	±0.3 °C
Pressure	±0.2 bar
Mass flux	±0.125 kg/h
Heat flux	±7 W
Diameter	±0.007 mm

Table 2. Partial experimental uncertainties

3. EXPERIMENTAL RESULTS

3.1 The results for turbuliser T1

The effect of mass flux and heat flux

Figure 3 shows the relation between the average measured heat transfer coefficient on the tube length and the mass flux, *G*, for the tube of 2.3 mm inner diameter. It can be seen that heat transfer coefficient depends on the mass flux when all of the other parameters are fixed. In this case it can be seen that the heat transfer coefficient first decreases with increasing mass flux and then begins to raise after exceeding the value of G≈1600 kg/m^{2}s. This demonstrates the effect of the presence of turbulisers for larger mass velocities. In such case the convective mechanism of the flow boiling is dominating and the turbulisers start to show up their presence by introduction of turbulisation. For G<1600 kg/m^{2}s the contribution of convective heat exchange in the total heat transport is significant and the mechanisms similar to nucleate boiling don’t have dominant character. This is in agreement with the smooth tube case [4]. In figures 4 – 8 distributions of heat transfer coefficient in terms of heat flux are presented. For

the low qualities we obtain the maximum of heat transfer coefficient value and then its gradual decrease with increasing of vapour content in the flow. The most of the data was registered for low inlet qualities, what is the reason for nucleate boiling domination in this area. The higher values of inlet quality could cause dryout, which is not a subject of present work.

When analysing the heat exchange with turbuliser T1 installed it can be noticed that heat transfer coefficient values become constant for quality ranging from 0.3 to 0.4. Much results resemble the laminar flow character. This phenomena should be further analysed. Because of the lack of experimental data for the higher qualities, authors not assumed the second heat transfer coefficient maximum existence, however, on the other hand, it cannot be completely excluded. Some increasing trends in heat transfer coefficient are noticeable.

Fig. 3. Average heat transfer coefficient as a function of mass flux, turbuliser T1, D=2.3mm.

Fig. 4. Effect of heat flux on the local heat transfer coefficient in function of quality, turbuliser T1, G=810 kg/(m^{2}s).

Fig. 5. Effect of heat flux on the local heat transfer coefficient in function of quality, turbuliser T1, D=2.3mm, G=935 kg/(m^{2}s).

Fig. 6. Effect of heat flux on the local heat transfer coefficient in function of quality, turbuliser T1, D=2.3mm, G=995 kg/(m^{2}s).

Fig. 7. Effect of heat flux on the local heat transfer coefficient in function of quality, turbuliser T1, D=2.3mm, G=1140 kg/(m^{2}s).

Fig. 8. Effect of heat flux on the local heat transfer coefficient in function of quality, turbuliser T1, D=2.3mm, G=1665 kg/(m^{2}s).

Figures from 9 to 11 shows measured heat transfer coefficient as a function of local quality at constant values of heat fluxes and variable mass flux. The results shows that the maximum of the heat transfer coefficient exists and moves in the direction of lower qualities with increasing heat flux. Decreasing of the value of this maximum can also be noticed. Experimental series corresponding to the lowest mass fluxes, achieves the higher qualities on the test section outlet. Also in this case the existence of second heat transfer coefficient maximum can't be completely excluded.

Fig. 9. Effect of mass flux on the local heat transfer coefficient in function of quality, turbuliser T1, D=2.3mm, q=45754 W/m^2.

Fig. 10. Effect of mass flux on the local heat transfer coefficient in function of quality, turbuliser T1, D=2.3mm, q=51585 W/m^2

Fig. 11. Effect of mass flux on the local heat transfer coefficient in function of quality, turbuliser T1, D=2.3mm, q=57765 W/m^2.

Comparison with experiments without flow blockage

As presented in the introduction, many correlations for saturated flow boiling are available in literature. Naturally, these correlations are intended to be used for calculations of heat transfer mainly in smooth tubes. However, in practice there is often a necessity to make calculations for heat exchanger including turbulisers without having an adequate equation. The tube with turbuliser T1 is a good example. Then it seems to be useful to compare the experimental data acquired for the tube with turbulisers with the flow boiling correlations for smooth tubes. The results of such comparison are presented in figures 12 and 13 Three correlations from the literature were used, which are adequate for determination of flow boiling heat transfer in mini- and microchannels, namely: correlations due to Kandlikar and Steinke [5], Lazarek and Black [6] and Owhaib [7].

Lazarek and Black [6], measured the local and average heat transfer coefficient, pressure drop, and critical heat flux of saturated boiling of R113 flowing vertically upwards and downwards in 3.17 mm tubes, of the length L = 123 and 246 mm, G = 125–750 kg/(m^{2}s), p=1.3–4.1 bar, q_w = 14–380 kW/m^2, and $\Delta T_{sub,in}$ = 3–73 K. The heat transfer coefficient was

found to be independent of x for $x \geq 0$. They presented an empirical correlation for local saturated boiling heat transfer coefficients, where the Nusselt number is a function of the liquid Reynolds number and the boiling number.

$$\alpha_{TPB} = 30\left(\mathrm{Re}_{LO}\right)^{0.857} Bo^{0.714} \frac{\lambda}{d} \tag{7}$$

Steinke and Kandlikar [5] recommend that in the case of Reynolds number smaller than 1600, i.e. $\mathrm{Re}_{LO} < 1600$, the heat transfer coefficient α_{LO} should be determined from the laminar flow range correlations, such as in case of constant heat flux, $\mathrm{Nu}_{LO}=4.36$. The two-phase flow heat transfer coefficient α_{TPB} is a greater value of the two α_{NBD} or α_{CBD}:

$$\alpha_{NBD} = 0.6683 Co^{-0.2} \alpha_{LO} + 1058.0 Bo^{0.7} F_{fl} \alpha_{LO} \tag{8a}$$

$$\alpha_{CBD} = 1.1360 Co^{-0.9} \alpha_{LO} + 667.2 Bo^{0.7} F_{fl} \alpha_{LO} \tag{8b}$$

The parameter F_{fl} is a fluid dependent factor, describing the pool boiling. It can be read from relevant tables for different fluids.

Owhaib [7] studied flow boiling of R134a in a test section of diameter 1,700, 1,224 and 0.826 mm. His results were fitted by the empirical expression:

$$\alpha_{TPB} = 400\left(\mathrm{Re}_{LO}\, Bo\right)^{0,5} \left(1 - x_e\right)^{0,1} Con^{0,55} p_r^{1,341} \left(\frac{\rho_l}{\rho_g}\right)^{0,37} \frac{\lambda_l}{d} \tag{9}$$

In (9) x_e denotes the vapour quality at outlet from the test section.

Results obtained using these correlations were compared with the results of application of the correlation due to Mikielewicz et al [8], in which the two phase multiplier was defined using the modified equation of Muller-Steinhagen and Heck [9] or Tran at al. [10], which reads:

$$\frac{\alpha_{TPB}}{\alpha_{LO}} = \sqrt{\left(R\right)^n + \frac{C}{1+P}\left(\frac{\alpha_{PB}}{\alpha_{LO}}\right)^2} \tag{10}$$

In equation (10) C=1 in case of flow boiling modeling and C=0 for flow condensation, the term $P = 2.53\times10^{-3}\,\mathrm{Re}_{LO}^{1.17}\, Bo^{0.6}\left(R_{MS}-1\right)^{-0.65}$. The pool boiling heat transfer coefficient α_{PB}, is recommended to be calculated from the relation due to Cooper [11]. The applied heat flux is incorporated through the boiling number Bo, defined as, $Bo=q/(Gh_{lv})$. In correction P, present in (10), the two-phase flow multiplier due to Muller-Steinhagen and Heck [9] must be used, as that model was utilised in the procedure of data reduction and determination of the regression coefficients. Here it acts in the correction P as a sort of the convective number. In order to

attain that the two-phase flow multiplier model due to Muller-Steinhagen and Heck [9] was modified to incorporate the function f_{1z}, which secures such limiting behavior. The resulting expression now reads:

$$R_{MS} = \left[1 + 2\left(\frac{1}{f_1} - 1\right)x\right] \cdot (1-x)^{1/3} + x^3 \frac{1}{f_{1z}} \tag{11}$$

In equation (11) $f_1=(\rho_L/\rho_G)\ (\mu_L/\mu_G)^{0.25}$ for turbulent flow and $f_1=(\rho_L/\rho_G)(\mu_L/\mu_G)$ for laminar flows. Introduction of the function f_{1z}, expressing the ratio of heat transfer coefficient for liquid only flow to the heat transfer coefficient for gas only flow, is to meet the limiting conditions, i.e. for x=0 the correlation should reduce to a value of heat transfer coefficient for liquid, $\alpha_{TPB}=\alpha_L$ whereas for x=1, approximately that for vapour, i.e. $\alpha_{TPB}\cong\alpha_G$. Hence:

$$f_{1z} = \frac{\alpha_G}{\alpha_L} \tag{12}$$

where $f_{1z}=(\lambda_G/\lambda_L)$ for laminar flows and for turbulent flows $f_{1z}=(\mu_G/\mu_L)(\lambda_L/\lambda_G)^{1.5}(c_{pL}/c_{pG})$.
Also the influence of chosen method of single-phase heat transfer coefficient calculation is also shown on the performance of that correlation. Two methods were used for this calculation: Dittus-Boelter [12] and Petukhov [13].
Dittus-Boelter correlation (1930):

$$Nu = 0.023\,\mathrm{Re}^{0.8}\,\mathrm{Pr}^{n} \tag{13}$$

In (13) n is set to 0.3 in case of cooling of the flow and 0.4 for heating. Correlation is applicable for $Re \geq 10^4$, $0.7 \leq Pr \leq 160$, $L/D_i \geq 10$, where L is the tube length.

A more detailed correlation for fully developed turbulent flow was postulatem by Petukhov et al. (1973) [13]. The correlation has accuracy of heat transfer coefficient determination on the level of ±10% for the range of variation of Reynolds number and Prandtl number respectively: $4\cdot10^3 \leq Re \leq 10^6$, $0.5 \leq Pr \leq 10^6$.

$$Nu = \frac{\frac{f}{8}\cdot \mathrm{Re}\cdot \mathrm{Pr}}{\chi + 12{,}7\sqrt{\frac{f}{8}}\cdot\left(\mathrm{Pr}^{\frac{2}{3}} - 1\right)} \tag{14}$$

where: $f = \left[1{,}82 \cdot \log 10\left(\frac{\mathrm{Re}}{8}\right)\right]^{-2}$; $\chi = 1{,}07 + \frac{900}{\mathrm{Re}} - \frac{0{,}63}{1+10\cdot\mathrm{Pr}}$

Generally use of the Dittus-Boelter correlation returns better consistency with experimental data. Examination of the results in fig. 12 and 13 shows that the Lazarek and Black's and Owhaib's correlations reveal the heat transfer trends with flow blockage best. Practically the other correlations describe the experimental data properly only in few cases.

Fig. 12. Comparison of various correlations with in-house experimental data in function of quality, turbuliser T1, G=761 kg/m^{2}s, q=37136 W/m^2, D=2.3mm.

Fig. 13. Comparison of various correlations with in-house experimental data in function of quality, turbuliser T1, G=1056 kg/m^{2}s, q=68387 W/m^2, D=2.3mm.

Comparison with the correlation for small tubes

Figures 14 and 15 present experimental values of heat transfer coefficient compared with theoretical values determined using equation (10). An intention of making such a comparison was to examine how the existing empirical correlations predict the heat transfer coefficients for the case of heat transfer intensification. It appears that over 17% of measurements is contained in ±30% error limits and about 40% is contained in ±50% error limits. For the qualities x>0.3 an error level increases distinctly and also the increasing overprediction of heat transfer coefficient by correlation (10) can be noticed (fig. 15).

Fig. 14. Experimental heat transfer coefficient in function of theoretical heat transfer coefficient calculated from equation (10), turbuliser T1, D=2.3mm.

Fig. 15. Effect of the ratio of experimental heat transfer coefficient to theoretical (equation (10)) in function of quality, turbuliser T1, D=2.3mm.

3.2 The results for turbuliser T2

The effect of mass flux and heat flux

Figure 16 shows the relation between the average measured heat transfer coefficient on the tube length and the mass flux, *G*, for the tube of 2.3 mm inner diameter where the influence of turbuliser T2 is examined. Also in this case it can be seen that heat transfer coefficient depends on the mass flux when all of the other parameters are established. In this case it can be seen that the heat transfer coefficient first decreases with increasing mass flux. A significant participation of the convective single-phase heat transfer in total heat transport can also be seen. Mechanisms associated with nucleate boiling don't have dominant character, similarly to the smooth tube case. From figures 17 – 21 it can be concluded that heat transfer coefficient also depends on heat flux similarly as in the case of T1 turbuliser.

The most of the data were registered for low inlet qualities however some increasing trend can be noticed, which can potentially lead to the second heat transfer coefficient maximum. It can be concluded that heat transfer coefficient achieves it's maximum value for low qualities and then decreases with further quality increasing. Hence the existence of the second heat transfer coefficient maximum cannot be excluded.

Fig. 16. Average heat transfer coefficient in function of mass flux, turbuliser T2, D=2.3mm.

Fig. 17. Effect of heat flux on the local heat transfer coefficient in function of quality, G=805 turbuliser T2, kg/(m^{2}s).

Fig. 18. Effect of heat flux on the local heat transfer coefficient in function of quality, turbuliser T2, D=2.3mm, G=940 kg/(m^{2}s).

Fig. 19. Effect of heat flux on the local heat transfer coefficient in function of quality, turbuliser T2, D=2.3mm, G=1175 kg/(m^{2}s).

Fig. 20. Effect of heat flux on the local heat transfer coefficient in function of quality, turbuliser T2, D=2.3mm, G=1542 kg/(m^{2}s).

Fig. 21. Effect of heat flux on the local heat transfer coefficient in function of quality, turbuliser T2, D=2.3mm, G=1890 kg/(m^{2}s).

Figures from 22 to 24 show measured heat transfer coefficient in function of local quality at established constant heat fluxes and variable mass flux. Also in this case the results show that the maximum of the heat transfer coefficient exists and moves in the direction of lower qualities with increasing value of heat flux. Decreasing of the value of this maximum can also be noticed. In the case of microchannels, full or partial dryout is more probable at lower qualities than for conventional diameters, however the appearance of the second heat transfer coefficient maximum is possible.

Fig. 22. Effect of mass flux on the local heat transfer coefficient in function of quality, turbuliser T2, D=2.3mm, q=36173 W/m^2.

Fig. 23. Effect of mass flux on the local heat transfer coefficient in function of quality, turbuliser T2, D=2.3mm, q=52793 W/m^2

Fig. 24. Effect of mass flux on the local heat transfer coefficient in function of quality, turbuliser T2, D=2.3mm, q=60370 W/m^2.

Comparison with experiments without flow blockage

Similarly to the case of turbuliser T1, the experimental results were compared with the number of correlations available in the literature for smooth tubes. The results of this comparison are presented in figures 25 and 26. It can be noticed that the Lazarek and Black's correlation performs best in prediction of experimental data also in this case. The correlation (10), in which the Tran and other's model was used for the flow resistance description, also gives satisfactory prediction of experimental data.

Fig. 25. Comparison of various correlations with own experimental data in function of quality, turbuliser T2, G=995 kg/m^{2}s, q=61651 W/m^2, D=2.3mm.

Fig. 26. Comparison of various correlations with own experimental data in function of quality, turbuliser T2, G=1860 kg/m^{2}s, q=36675 W/m^2, D=2.3mm.

Figures 27 and 28 present experimental results compared with theoretical values of heat transfer coefficient determined from the correlation due to Mikielewicz et al. along with the

Dittus-Boelter correlation for liquid only flow. It appears that over 18% of measurements is contained in ±30% error limits and about 30% is contained in ±50% error limits. Similarly to the T1 turbuliser, this error isn't spread uniformly for all qualities (fig. 28) and it also depends on the mass flux G. At a first glance the error characteristics are similar to the case of T1 turbuliser.

For the qualities x>0.3 an error level increases distinctly and also the increasing overprediction of heat transfer coefficient by the correlation (10) can be noticed, (fig. 28).

Fig. 27. Experimental heat transfer coefficient in function of theoretical heat transfer coefficient calculated from equation (10), turbuliser T2, D=2.3mm.

Fig. 28. Effect of experimental heat transfer coefficient on theoretical heat transfer coefficient (equation (10)) in function of quality, turbuliser T2, D=2.3mm.

Generalized comparison of heat transfer intensification methods

It's difficult to precisely valuate if the specific flow turbulising method really improves heat transfer or not. To estimate it, the equation (6) was used, which is based on the pumping power and heat transferred through the channel. The results obtained for the constant quality at the section output are presented in the figures 29, 31, 33 and 35. The turbulisation effect isn't noticeable. Regardless of used turbuliser (T1 or T2), the heat transfer is worse than in the case of smooth tube. It's quite a surprising result as some positive effect was rather expected. In figures 30, 32, 34 and 36 the heat quantities, possible to be transferred in specific configuration, are presented in relation to the pumping power. Also in this interpretation it can be seen that smooth tube is better than T1 or T2 turbuliser.

The values of E coefficient were drawn for both variants of turbulisation. It can be concluded, that the improvement of heat transfer occurs for the moderate and high qualities but for the low qualities insertion of the mechanical turbulisers didn't brought expected results. This can be explained by higher qualities which occur in the turbulised tube, in comparison with the smooth one, for the same heat flux. Referring to the heat transfer coefficient curve as the function of quality, it can be noticed, that heat transfer coefficient values are smaller for higher qualities. This corresponds with the conclusions from experimental data analysis for the case of turbulisation.

The second possible explanation of the lack of intensification in presented cases is the flow laminarisation as an effect of blocking the significant part of channel diameter by the turbuliser. Boiling during the laminar flow is characterized by the lower heat transfer coefficient values. Some calculations were carried out using the Mikielewicz's model (10) for the values of Reynolds number Re=700. The heat transfer coefficient obtained using that correlation for laminar flow was 950 W/m^{2}K. On the other hand a value of heat transfer coefficient 2240 W/m^{2}K was obtained using the correlation with turbulent flow properties. This proves that the heat transfer coefficient for the laminar flow is considerably lower.

Fig. 29. Heat removed by the working medium in function of pumping power in case of considered turbulisers T1 and T2, x=0.3, D=2.3mm.

Fig. 30. Relation between the heat removed by the working medium and the pumping power in case of considered turbulisers T1 and T2, x=0.3, D=2.3mm

Fig. 31. Heat removed by the working medium in function of pumping power in case of considered turbulisers T1 and T2, x=0.4, D=2.3mm.

Fig. 32. Relation between the heat removed by the working medium and the pumping power in case of considered turbulisers T1 and T2, x=0.4, D=2.3mm

Fig. 33. Heat removed by the working medium in function of pumping power, x=0.6 in case of considered turbulisers T1 and T2, D=2.3mm.

Fig. 34. Relation between the heat removed by the working medium and the pumping power in case of considered turbulisers T1 and T2, x=0.6, D=2.3mm

Fig. 35. Heat removed by the working medium in function of pumping power in case of considered turbulisers T1 and T2, x=0.8, D=2.3mm.

Fig. 36. Relation between the heat removed by the working medium and the pumping power in case of considered turbulisers T1 and T2, x=0.8, D=2.3mm.

Fig. 37. Comparison of intensification coefficients for the T1 turbuliser at various qualities.

Fig. 38. Comparison of intensification coefficients for the T2 turbuliser at various qualities.

4. CONCLUSIONS

This paper is an attempt to use turbulising inserts in minichannels during the flow boiling to achieve the heat transfer intensification. Two turbulisation variants were thoroughly verified experimentally. The framework of the experimental investigations contained experimental studies intended to obtain heat transfer intensification. Two different turbulisation inserts were taken into account. The intensification effect wasn't observed in most cases. The inserts filled the channel diameter to such a degree that the flow became laminar. This caused the lower heat transfer coefficient values. This result can also be interpreted as the transition of the flow to the higher quality ranges where heat transfer coefficient decreases, as the experiments for smooth tubes shown. Probably it's possible to obtain the intensification effect using the present inserts for low vapour content in the flow.

It was found that use of the turbulisers can have an influence on the localization of dryout. It can be useful in some cases, but dryout wasn't the subject of the present work. Widening of research onto other working fluids and channel diameters could contribute to explain the flow laminarisation phenomenon and to generalize obtained experimental results.

NOMENCLATURE

C - constant in equation (10)

D - channel inner diameter, m

E - heat transfer intensification coefficient

f - Fanning friction factor, functions in (11)

F - fluid dependent factor

G - mass flowrate, kg/m^{2}s

p - pressure, Pa

P - pumping power, W

$\dot{Q}$ - rate of heat,W

q - heat flux density, W/m^2

T - temperature, K

x - quality

R - two-phase flow multiplier

$\dot{V}$ - volumetric flow rate, m^3/s

x - vapour quality

$Bo = \frac{q}{G h_{lv}}$ - Boiling number

$Co = \left(\frac{1-x}{x}\right)^{0,8} \left(\frac{\rho_g}{\rho_l}\right)^{0,5}$ Convective number

$Nu = \frac{\alpha \cdot d}{\lambda}$ - Nusselt number

$\mathrm{Re} = \frac{G \cdot d}{\mu_L}$ - Reynolds number

α - heat transfer coefficient, W/m^2K

λ - thermal conductivity, W/mK

ρ - density

Δ - difference

Subscripts

CBD - convective boiling dominated region

e - exit from test section

g - gas

LO - liquid only

l - liquid

NBD - nucleate boiling dominated region

o - flow without blocking inserts

p - constant pumping power

PB - pool boiling

r - reduced conditions

SAT - saturation conditions

TPB - two-phase boiling

w - wall

REFERENCES

[1] Bergles A.E., 2001, ExHFT for fourth generation heat transfer technology, Experimental Thermal and Fluid Sciences, Vol. 26, pp. 325-334.
[2] Dewan A., Mahanta P., Raju K.S., Kumar P.S., 2004, Review of passive heat transfer augmentation techniques, Proc. Institution of Mechanical Engineers, 218, Part A: J. Power and Energy, 509-527.
[3] Eiamsa-ard S., Promvonge P., 2007, Heat transfer characteristics in a tube fitted with a helical screw-tape with/without core-rod inserts, Int. Comm. in Heat and Mass Transfer, 34, 176-185.
[4] Mikielewicz D., Klugmann M., Wajs J., 2012, Experimental investigation of M-shape heat transfer coefficient distribution of R123 flow boiling in small diameter tubes, Journal of Heat Transfer Engineering, vol. 33, issue 7, pp. 584-595.
[5] Steinke M.E., Kandlikar S., 2006, Single-phase liquid friction factors in microchannels, Int. J. of Thermal Sciences, Vol. 45, pp. 1073-1083.
[6] Lazarek G.M., Black S.H., 1982, Evaporative heat transfer, pressure drop and critical heat flux in a small vertical tube with R-113, Int. J. Heat Mass Transfer , Vol. 25, No. 7, pp. 945-960.
[7] Owhaib W., 2007, Experimental Heat Transfer, Pressure Drop and Flow Visualization of R134a in Vertical Mini/Micro Tubes, PhD dissertation, KTH, Stockholm, 2007.
[8] Mikielewicz D., Mikielewicz J., Tesmar J., 2007, Improved semi-empirical method for determination of heat transfer coefficient in flow boiling in conventional and small diameter tubes, Int. J. of Heat and Mass Transfer, 50, 3949-3956.
[9] Muller-Steinhagen R., Heck K., 1986, A simple friction pressure drop correlation for two-phase flow in pipes, Chem. Eng. Progress, 20, 297-308.
[10] Tran T.N., Wambsganss M.W., Chyu M.C. and France D.M., 1997, A correlation for nucleate flow boiling in small channels, In: Shah, R.K. (Ed), Compact Heat Exchanger for the Process Industries. Begell House, New York, pp. 353-363.
[11] Cooper M. G., 1984, Saturation nucleate pool boiling: a simple correlation, Int. Chem. Eng. Symposium 1, 86, 785-79.
[12] Dittus F. W., Boelter L.M.K., 1930, Heat transfer in automobile radiators of tubular type, University of California Pub. Eng., 2, 443-461.
[13] Petukhov B., Kurganov V., Gladuntsov A., 1973, Heat transfer in turbulent pipe flow of gases with variable properties, Heat Transfer Soviet Research, Vol. 5, pp. 109-116.

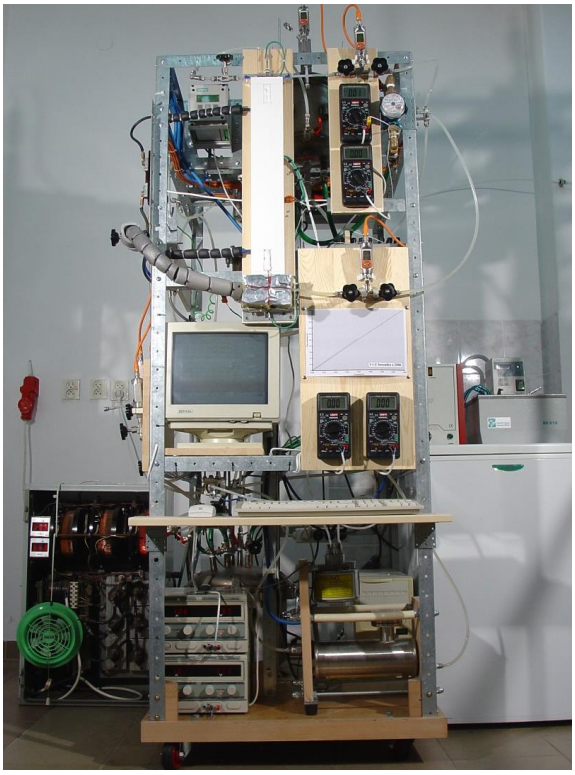

Figure 1. General view of experimental facility

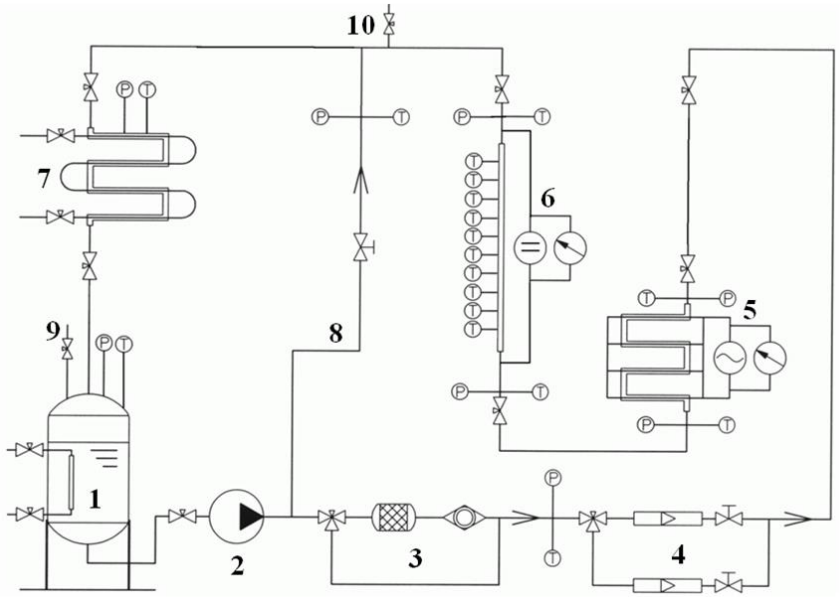

Figure 2. Schematic diagram of test facility: 1– main tank; 2 – pump section; 3 – filter/dryer; 4 – mass flowmeters; 5 –pre-heater; 6 – test section; 7 – condenser; 8 – by-pass; 9 – filling valve; 10 – de-aerator

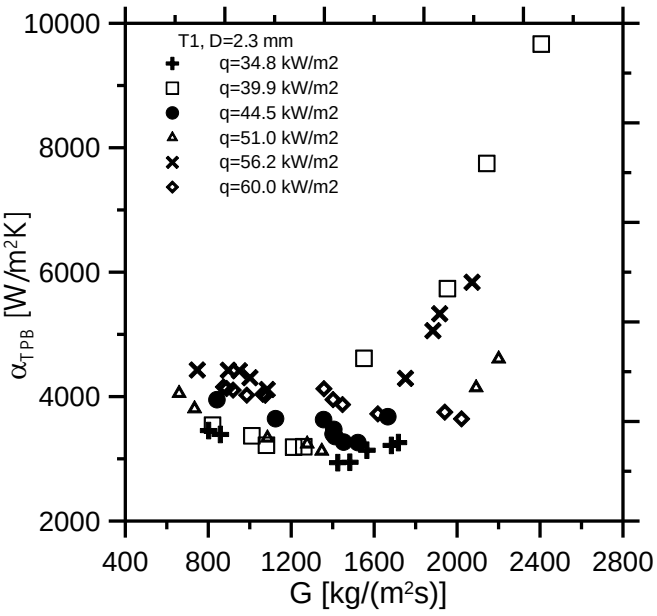

Fig. 3. Average heat transfer coefficient as a function of mass flux, turbuliser T1, D=2.3mm.

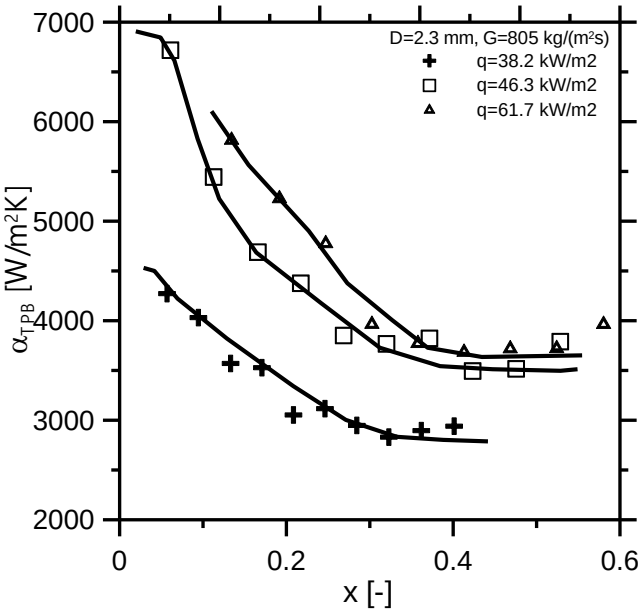

Fig. 4. Effect of heat flux on the local heat transfer coefficient in function of quality, turbuliser T1, G=810 kg/(m^{2}s).

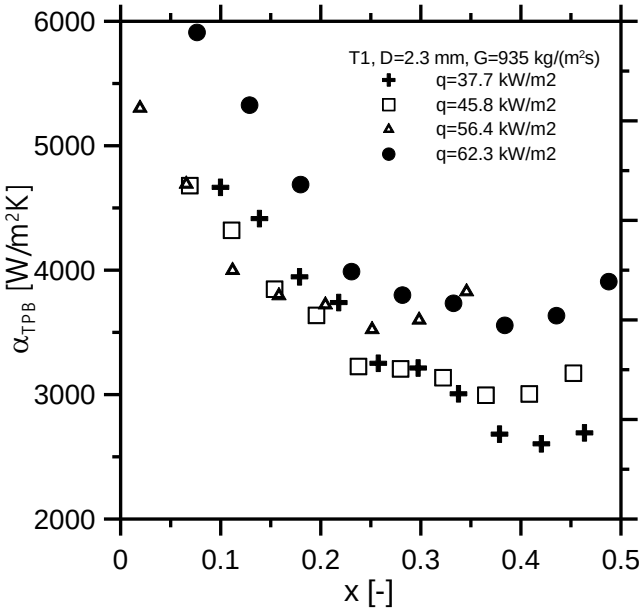

Fig. 5. Effect of heat flux on the local heat transfer coefficient in function of quality, turbuliser T1, D=2.3mm, G=935 kg/(m^{2}s).

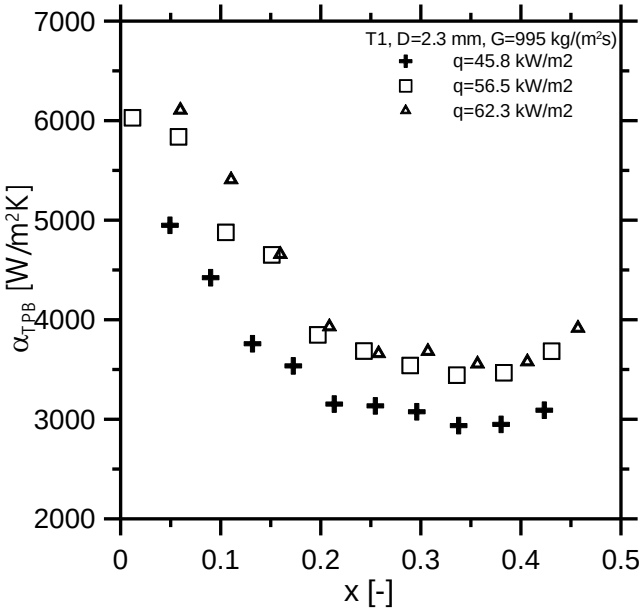

Fig. 6. Effect of heat flux on the local heat transfer coefficient in function of quality, turbuliser T1, D=2.3mm, G=995 kg/(m^{2}s).

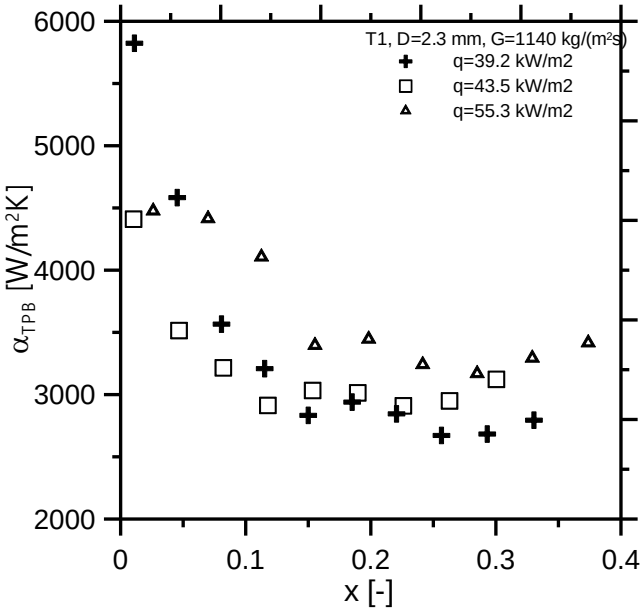

Fig. 7. Effect of heat flux on the local heat transfer coefficient in function of quality, turbuliser T1, D=2.3mm, G=1140 kg/(m^{2}s).

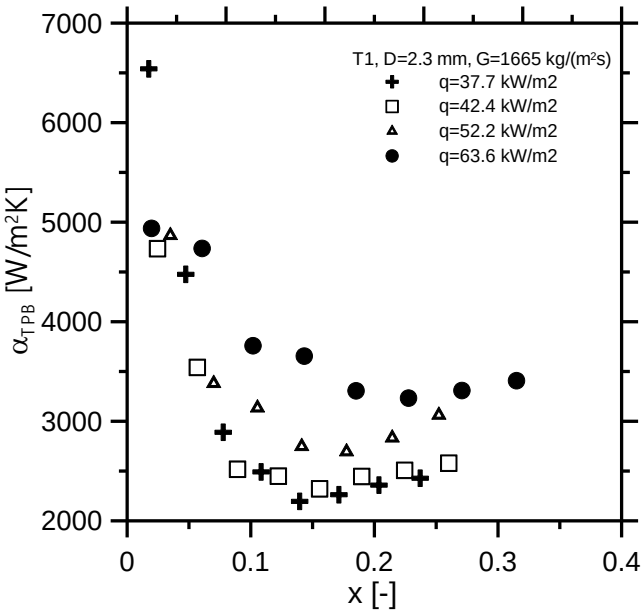

Fig. 8. Effect of heat flux on the local heat transfer coefficient in function of quality, turbuliser T1, D=2.3mm, G=1665 kg/(m^{2}s).

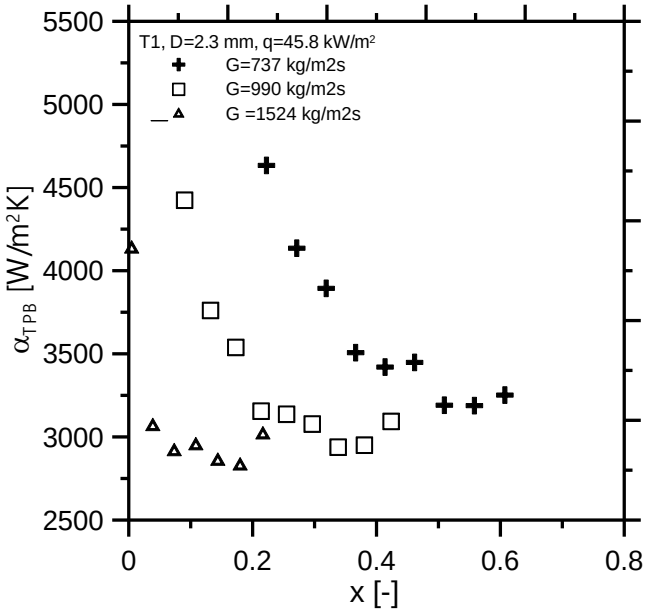

Fig. 9. Effect of mass flux on the local heat transfer coefficient in function of quality, turbuliser T1, D=2.3mm, q=45754 W/m^2.

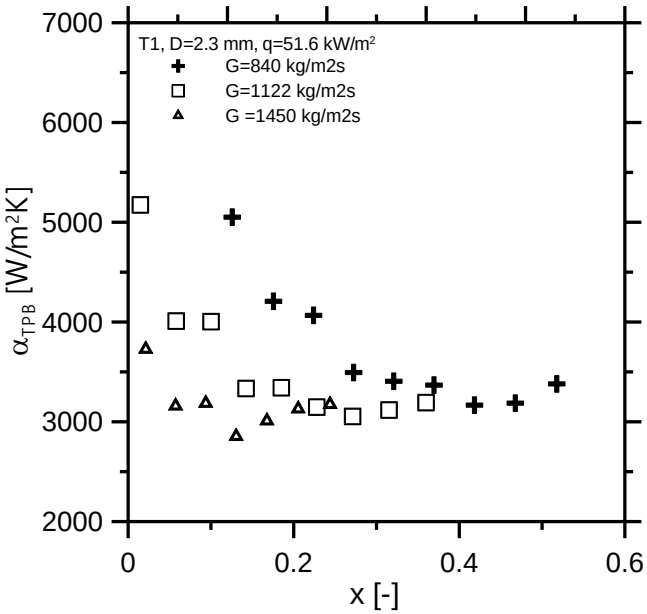

Fig. 10. Effect of mass flux on the local heat transfer coefficient in function of quality, turbuliser T1, D=2.3mm, q=51585 W/m^2

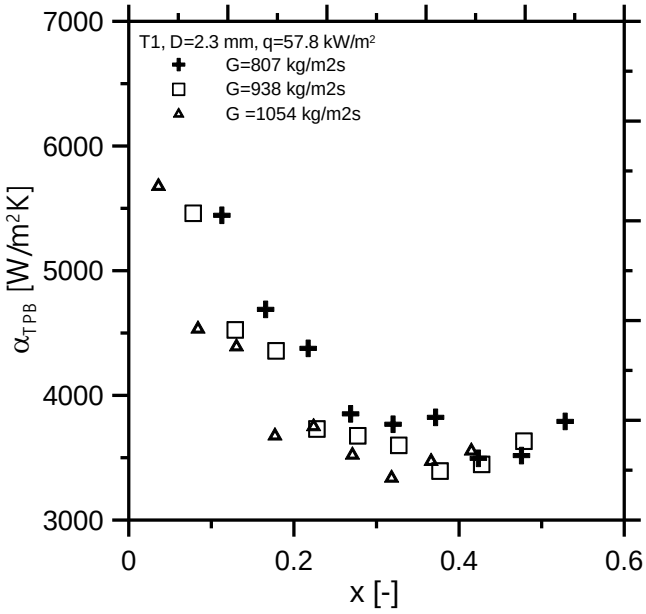

Fig. 11. Effect of mass flux on the local heat transfer coefficient in function of quality, turbuliser T1, D=2.3mm, q=57765 W/m^2.

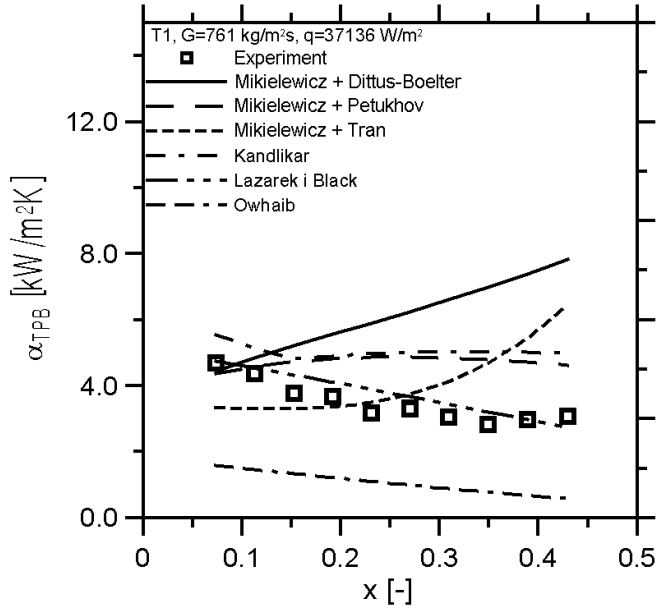

Fig. 12. Comparison of various correlations with in-house experimental data in function of quality, turbuliser T1, G=761 kg/m^{2}s, q=37136 W/m^2, D=2.3mm.

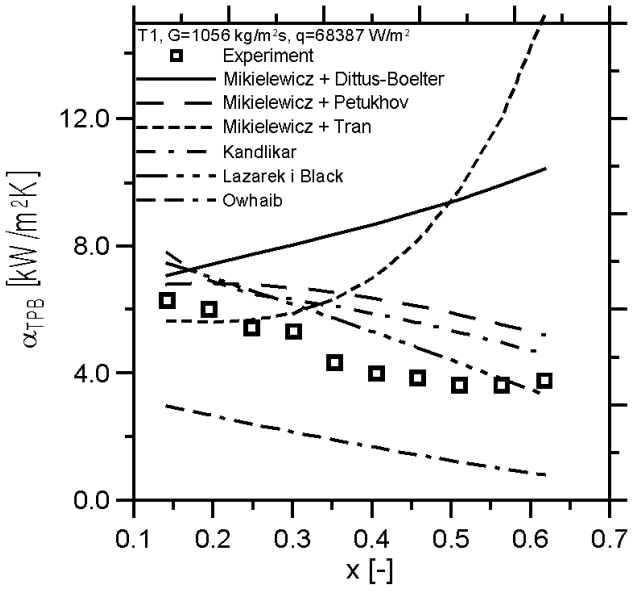

Fig. 13. Comparison of various correlations with in-house experimental data in function of quality, turbuliser T1, G=1056 kg/m^{2}s, q=68387 W/m^2, D=2.3mm.

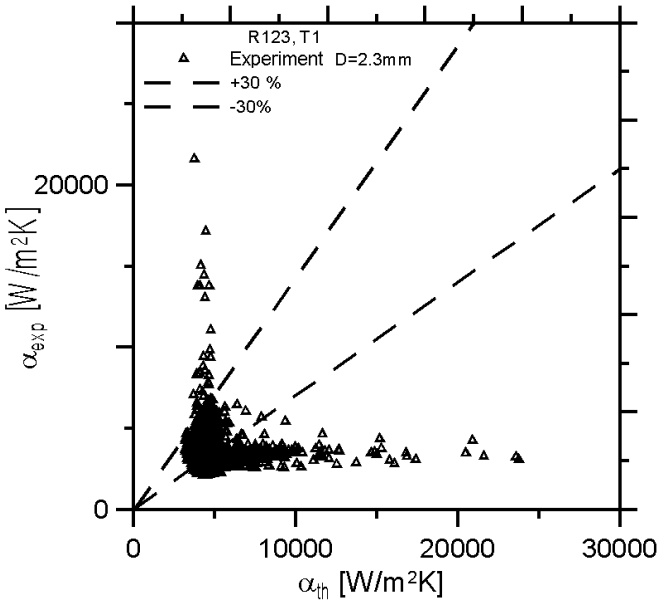

Fig. 14. Experimental heat transfer coefficient in function of theoretical heat transfer coefficient calculated from equation (10), turbuliser T1, D=2.3mm.

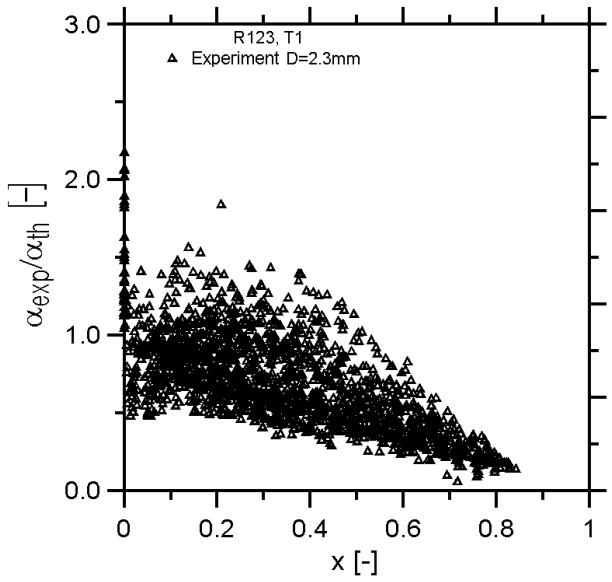

Fig. 15. Effect of the ratio of experimental heat transfer coefficient to theoretical (correlation (10)) in function of quality, turbuliser T1, D=2.3mm.

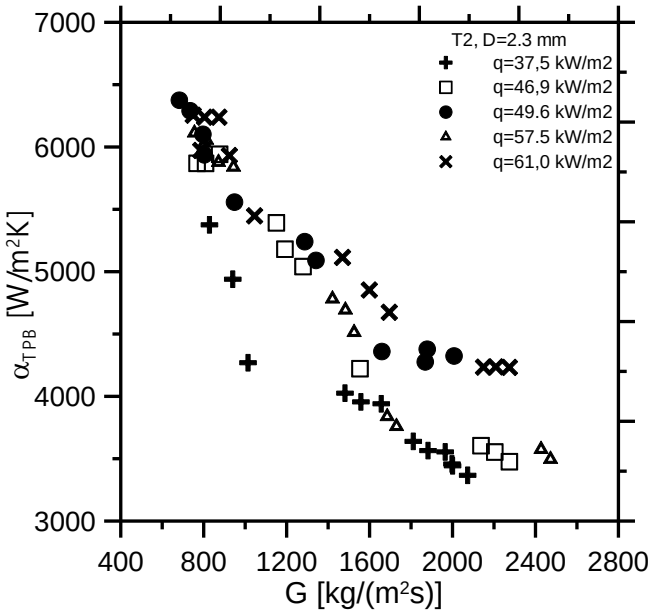

Fig. 16. Average heat transfer coefficient in function of mass flux, turbuliser T2, D=2.3mm.

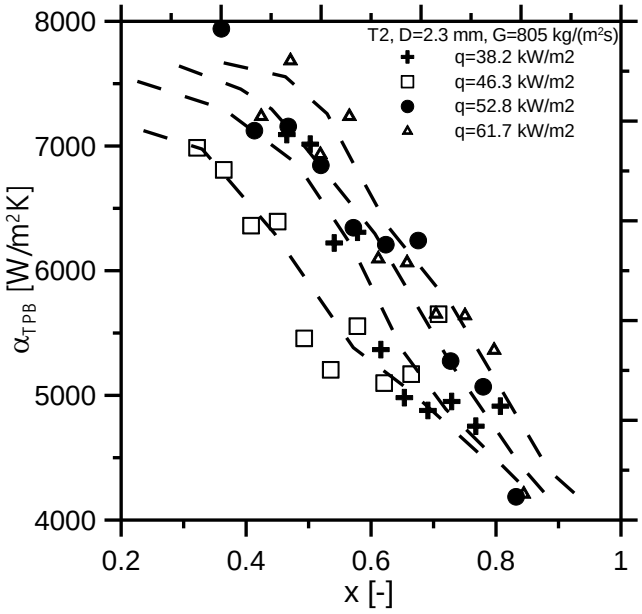

Fig. 17. Effect of heat flux on the local heat transfer coefficient in function of quality, turbuliser T2, G=805 kg/(m^{2}s).

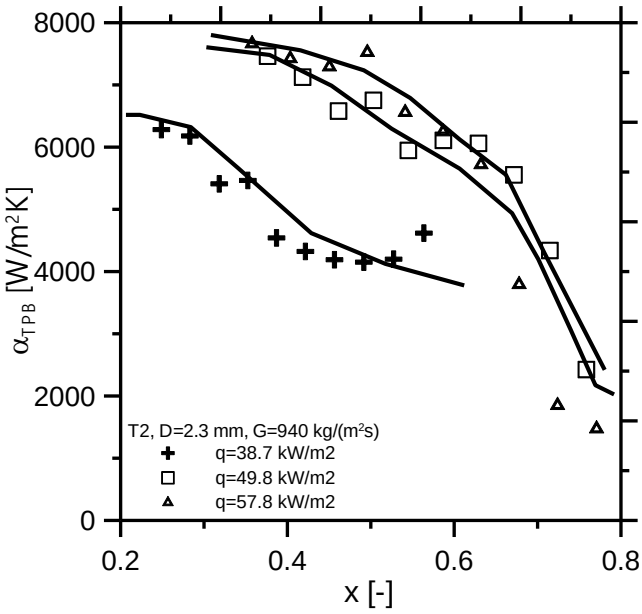

Fig. 18. Effect of heat flux on the local heat transfer coefficient in function of quality, turbuliser T2, D=2.3mm, G=940 kg/(m^{2}s).

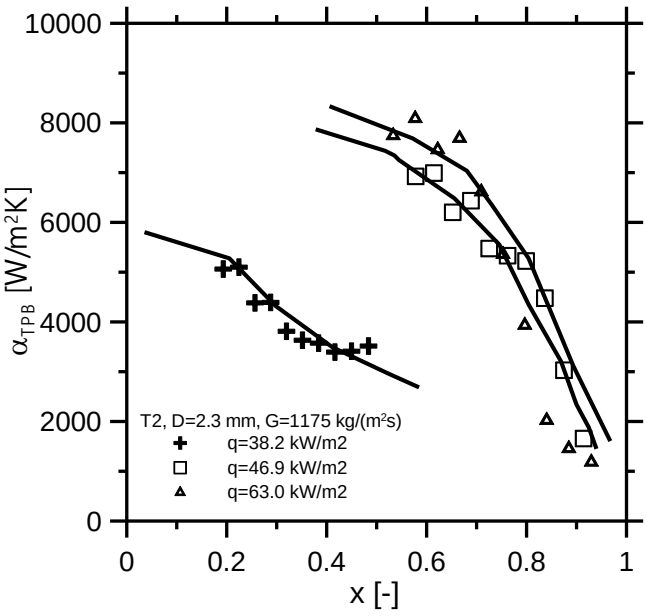

Fig. 19. Effect of heat flux on the local heat transfer coefficient in function of quality, turbuliser T2, D=2.3mm, G=1175 kg/(m^{2}s).

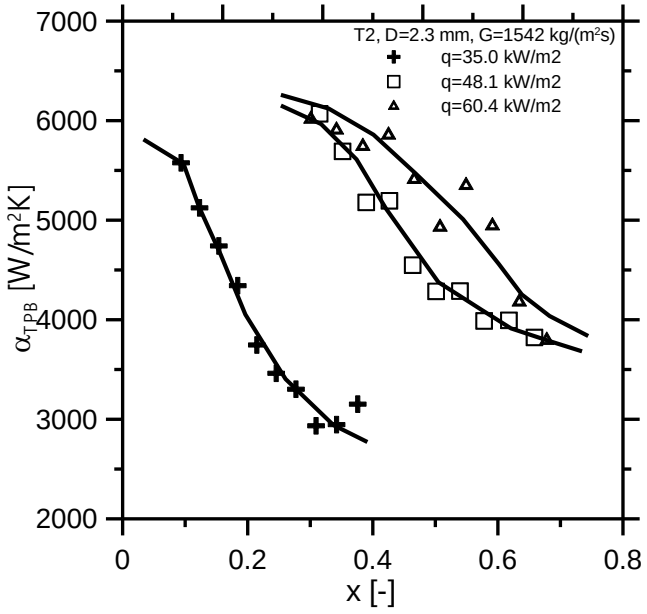

Fig. 20. Effect of heat flux on the local heat transfer coefficient in function of quality, turbuliser T2, D=2.3mm, G=1542 kg/(m^{2}s).

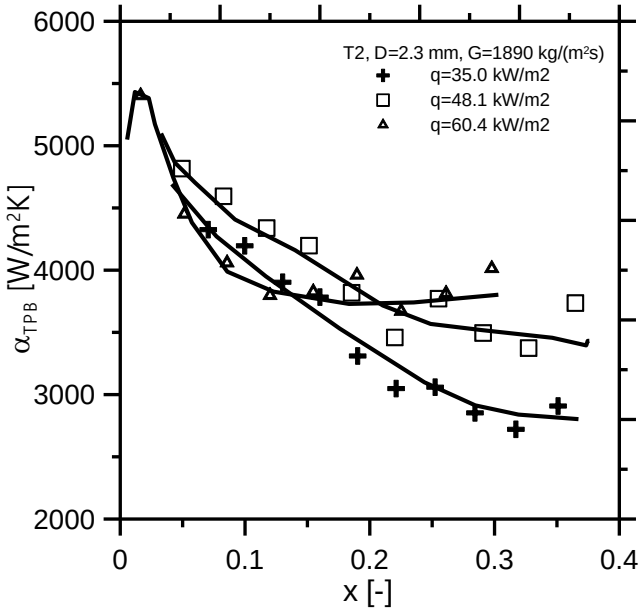

Fig. 21. Effect of heat flux on the local heat transfer coefficient in function of quality, turbuliser T2, D=2.3mm, G=1890 kg/(m^{2}s).

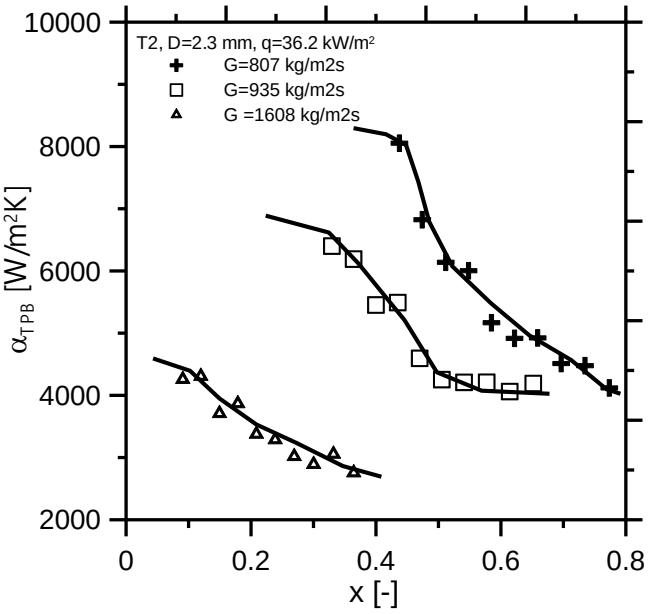

Fig. 22. Effect of mass flux on the local heat transfer coefficient in function of quality, turbuliser T2, D=2.3mm, q=36173 W/m^2.

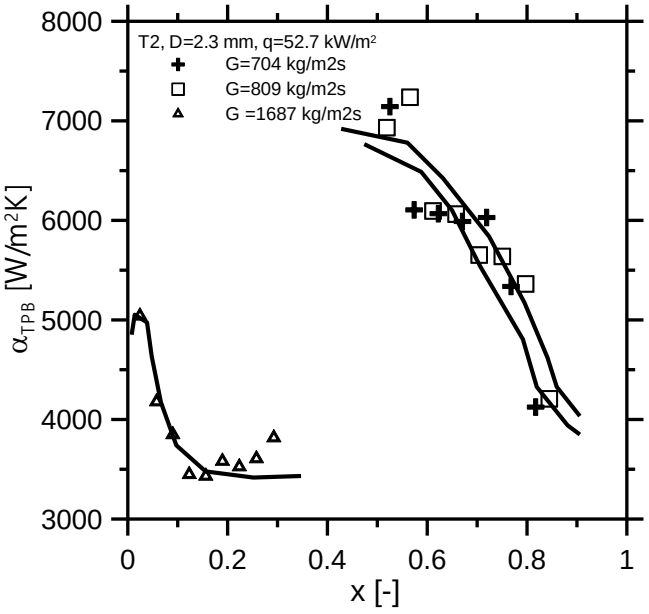

Fig. 23. Effect of mass flux on the local heat transfer coefficient in function of quality, turbuliser T2, D=2.3mm, q=52793 W/m^2

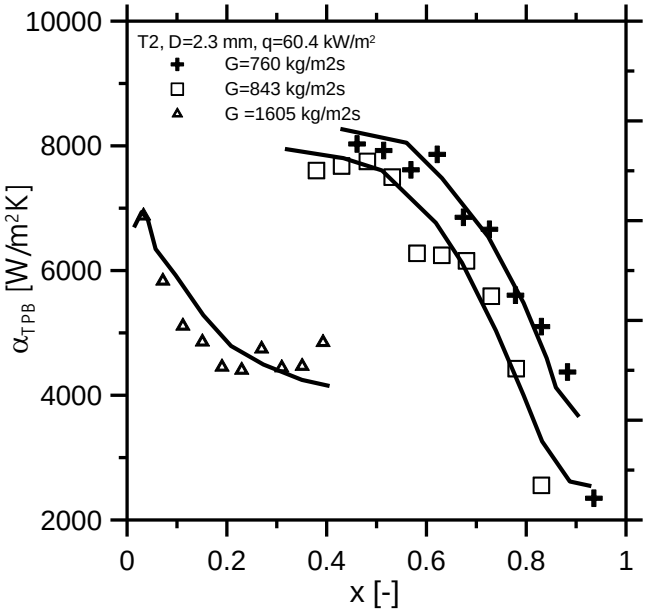

Fig. 24. Effect of mass flux on the local heat transfer coefficient in function of quality, turbuliser T2, D=2.3mm, q=60370 W/m^2.

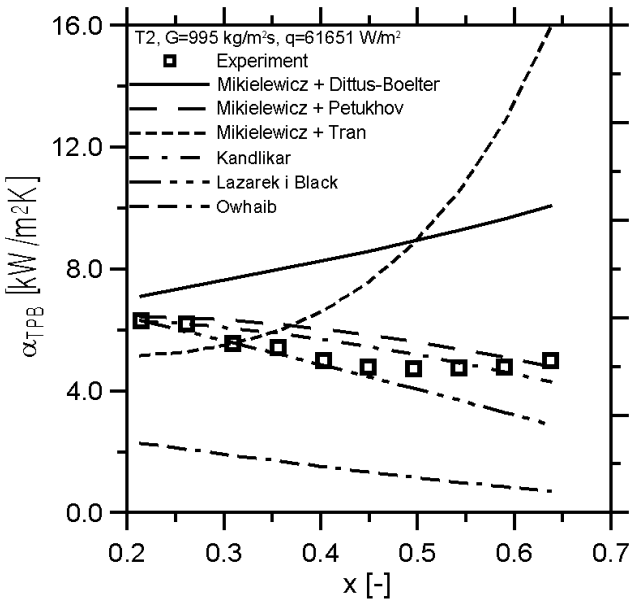

Fig. 25. Comparison of various correlations with own experimental data in function of quality, G=995 kg/m^{2}s, q=61651 W/m^2, D=2,3mm, turbuliser T2.

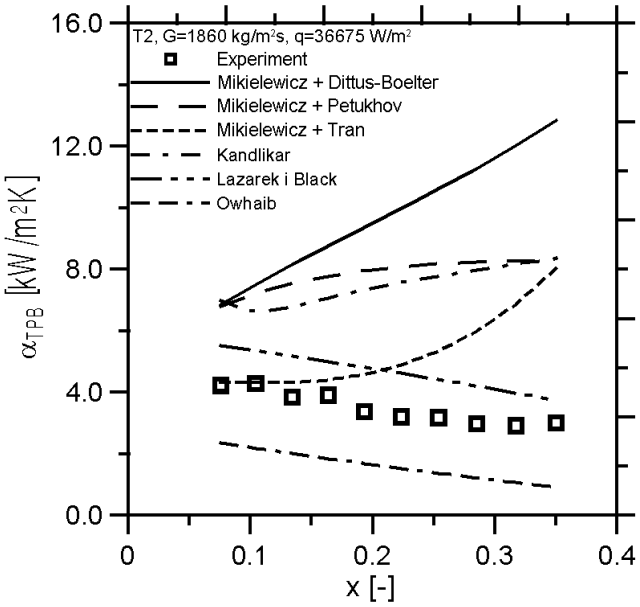

Fig. 26. Comparison of various correlations with own experimental data in function of quality, G=1860 kg/m^{2}s, q=36675 W/m^2, D=2,3mm, turbuliser T2.

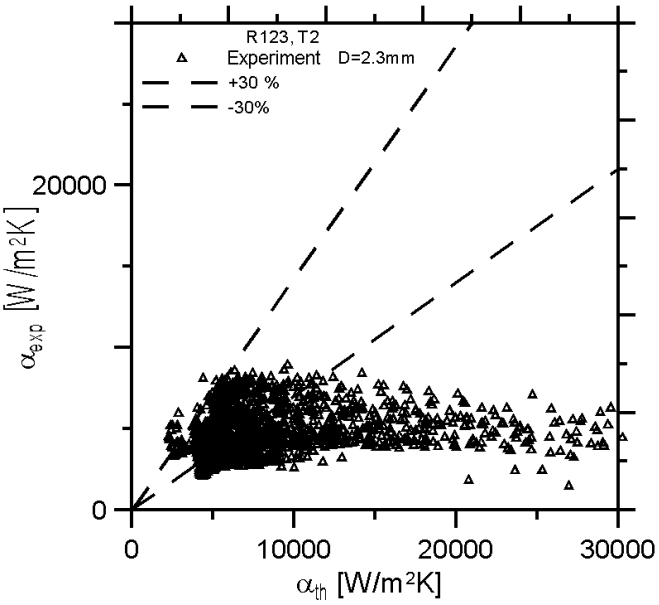

Fig. 27. Experimental heat transfer coefficient in function of theoretical heat transfer coefficient calculated from equation (10), D=2.3mm.

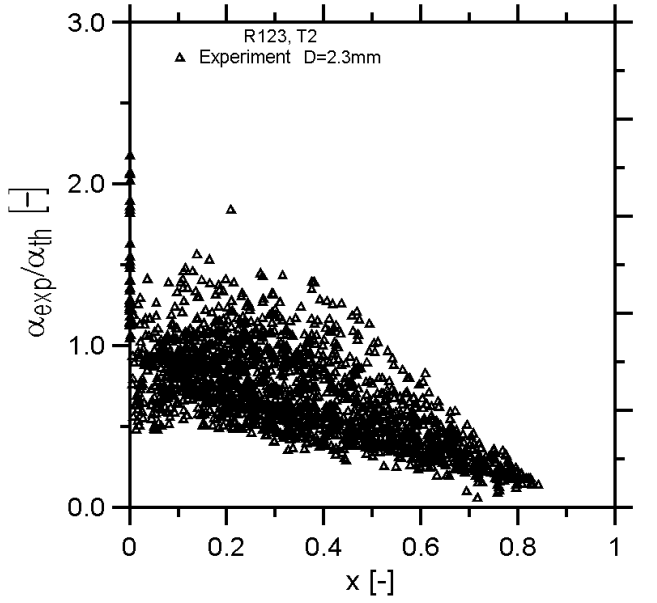

Fig. 28. Effect of experimental heat transfer coefficient on theoretical heat transfer coefficient (correlation (10)) in function of quality, D=2.3mm.

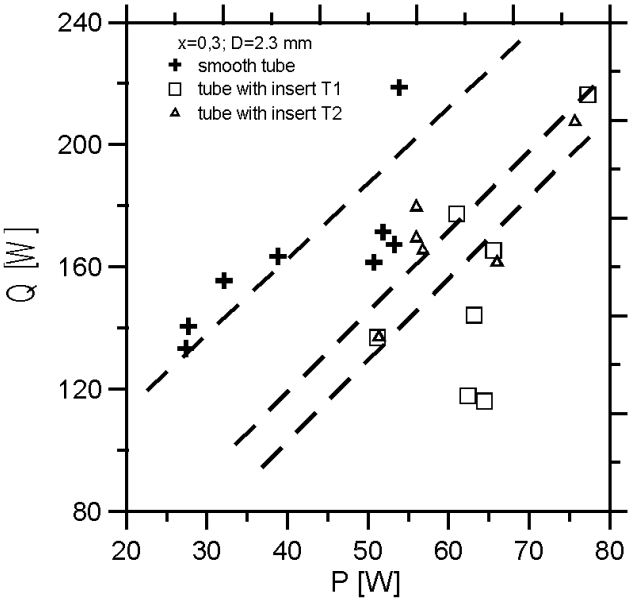

Fig. 29. Heat removed by the working medium in function of pumping power in case of considered turbulisers T1 and T2, x=0.3, D=2.3mm.

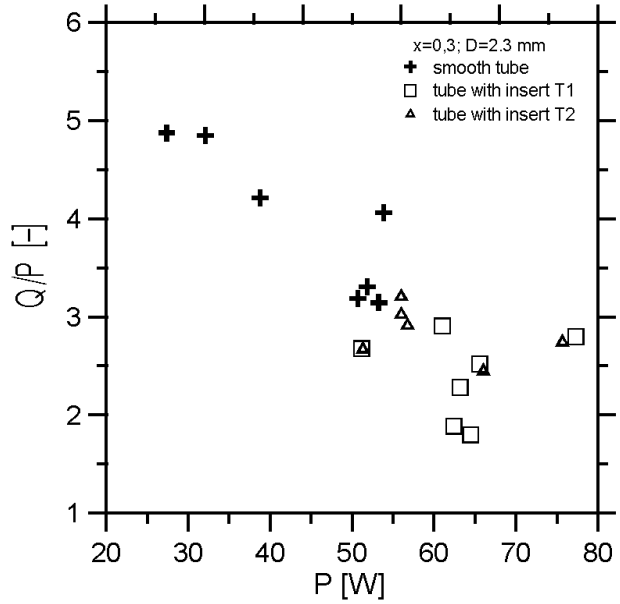

Fig. 30. Relation between the heat removed by the working medium and the pumping power in case of considered turbulisers T1 and T2, x=0.3, D=2.3mm

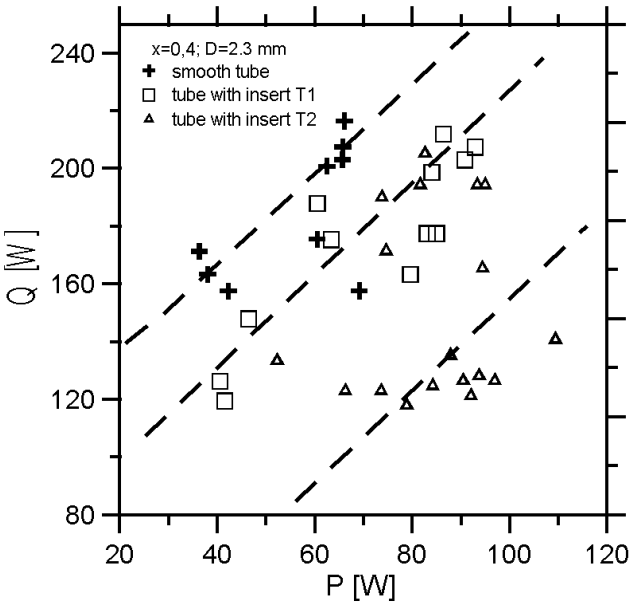

Fig. 31. Heat removed by the working medium in function of pumping power, x=0.4 in case of considered turbulisers T1 and T2, D=2.3mm.

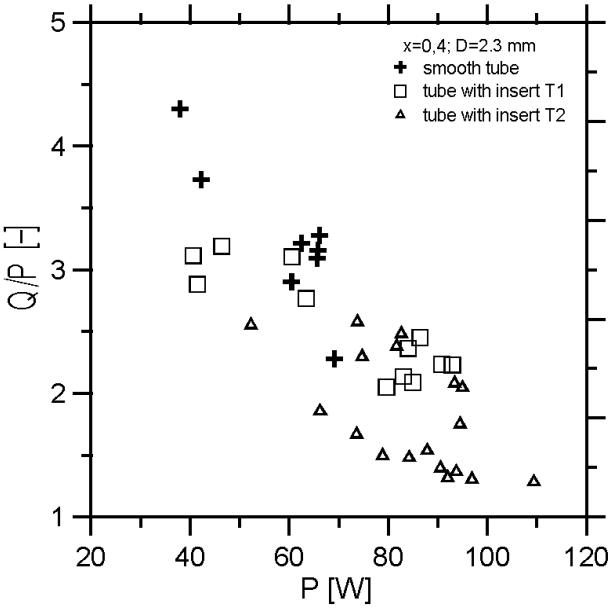

Fig. 32. Relation between the heat removed by the working medium and the pumping power in case of considered turbulisers T1 and T2, x=0.4, D=2.3mm

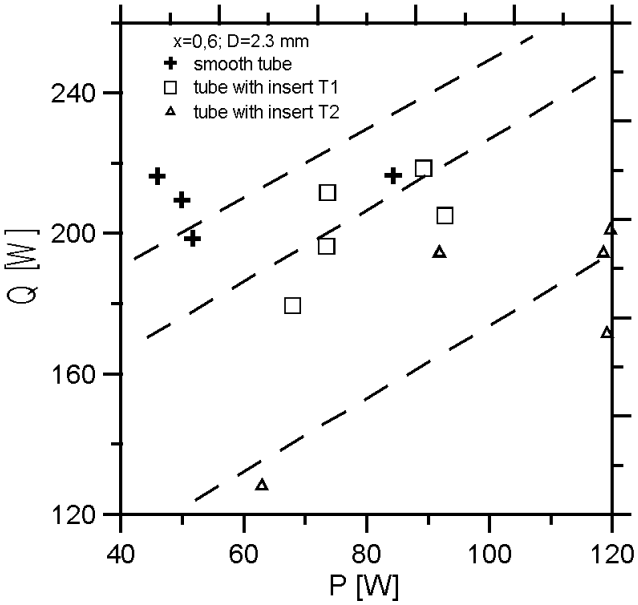

Fig. 33. Heat removed by the working medium in function of pumping power in case of considered turbulisers T1 and T2, x=0.6, D=2.3mm.

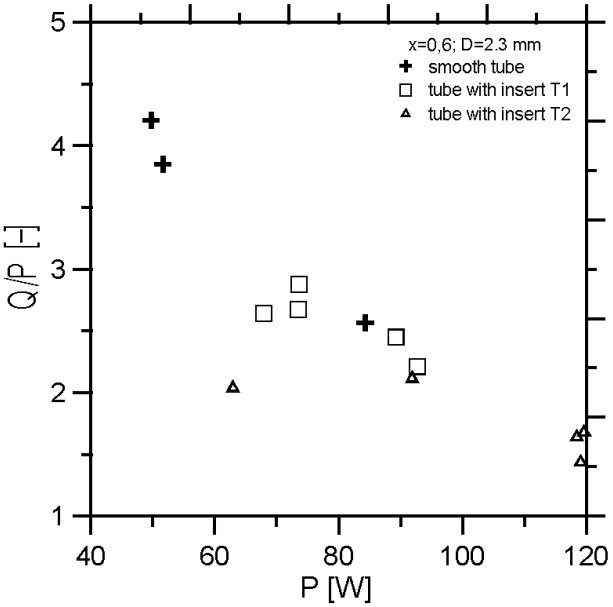

Fig. 34. Relation between the heat removed by the working medium and the pumping power in case of considered turbulisers T1 and T2, x=0.6, D=2.3mm

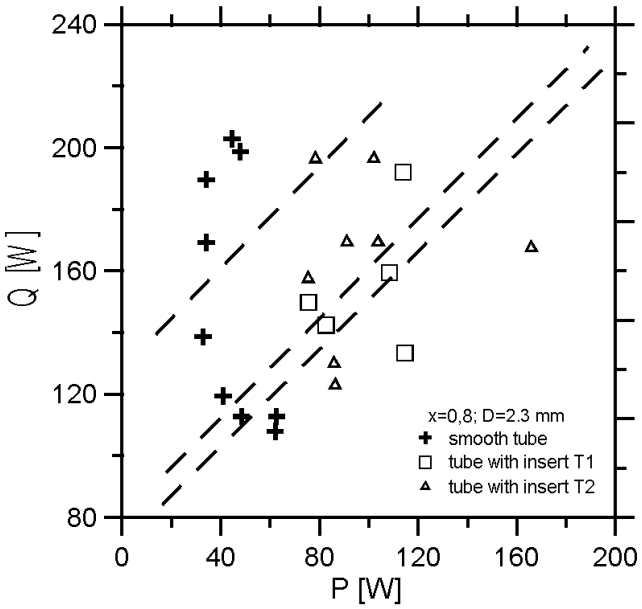

Fig. 35. Heat removed by the working medium in function of pumping power in case of considered turbulisers T1 and T2, x=0.8, D=2.3mm.

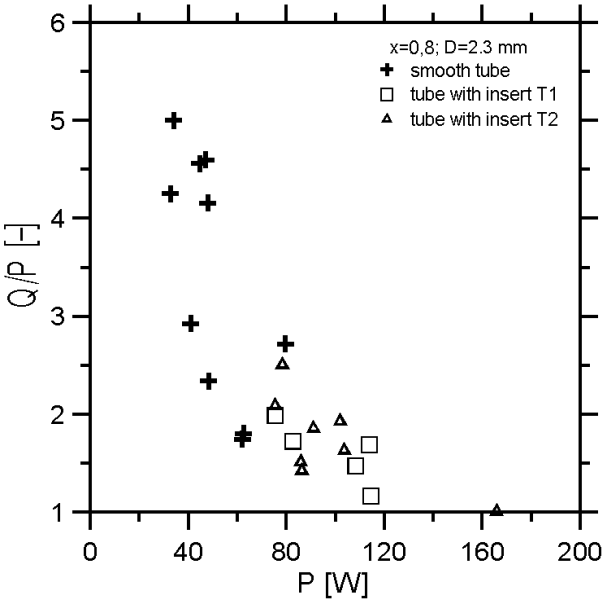

Fig. 36. Relation between the heat removed by the working medium and the pumping power in case of considered turbulisers T1 and T2, x=0.8, D=2.3mm.

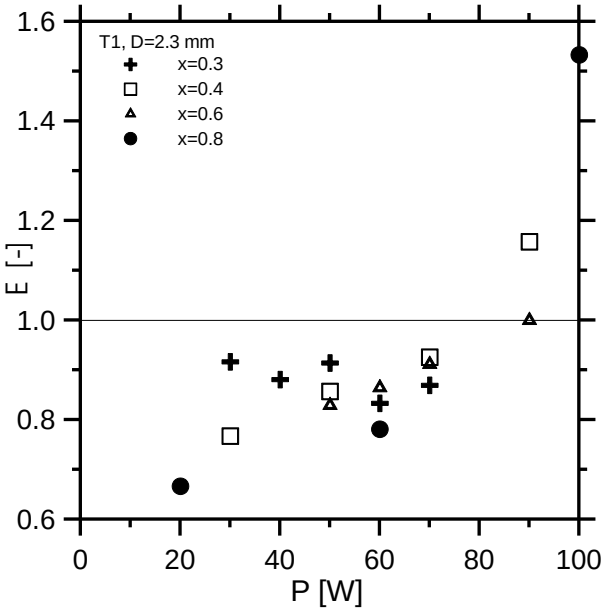

Fig. 37. Comparison of intensification coefficients for the T1 turbuliser at various qualities.

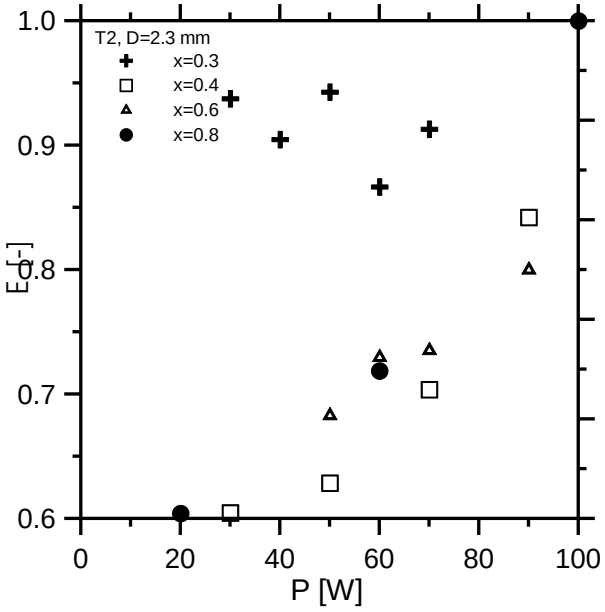

Fig. 38. Comparison of intensification coefficients for the T2 turbuliser at various qualities.